Z. Phys. A 351, 311–316 (1995)

ZEITSCHRIFT
FÜR PHYSIK A

$^{28}Si(^{32}S)$ fragmentation at 3.7 A, 14.6 A and 200 A GeV

M.I. Adamovich[12], M.M. Aggarwal[3], Y.A. Alexandrov[12], R. Amirikas[15], N.P. Andreeva[1], Z.V. Anzon[1], R. Arora[3], F.A. Avetyan[19], S.K. Badayal[7], A.M. Bakich[15], E.S. Basova[16], I.K. Bazarov[16], K.B. Bhalla[6], A. Bhasin[7], V.S. Bhatia[3], V.G. Bogdanov[14], V. Bradnova[5], V.I. Bubnov[1], T.H. Burnett[13], X. Cai[18], D.A. Carshiev[16], I.Y. Chasnikov[1], L.P. Chernova[17], M.M. Chernyavski[12], S. Dhamia[3], G.Z. Eligbaeva[1], L.E. Eremenko[1], A.S. Gaitinov[1], E.R. Ganssauge[11], S. Garpman[10], S.G. Gerassimov[12], C. Graf[11], J. Grote[13], K.G. Gulamov[17], S.K. Gupta[6], V.K. Gupta[7], B. Jakobsson[10], L. Just[8], S. Kachroo[7], G.S. Kalyachkina[1], E.K. Kanygina[1], M. Karabova[8], S. Kitroo[7], S.P. Kharlamov[12], A.D. Kovalenko[5], S.A. Karsnov[5], V. Kumar[6], V.G. Larionova[12], Y.D. Li[18], L.S. Liu[18], S. Lokanathan[6], J.J. Lord[13], N.S. Lukicheva[17], S.B. Luo[9], L.K. Mangotra[7], N.A. Marutyan[19], A.Y. Mashkov[17], N.V. Maslennikova[12], I.S. Mittra[3], S. Mokerjee[6], S.Z. Nasyrov[16], V.S. Navotny[17], J. Nystrand[10], M. Ochs[11], G.I. Orlova[12], I. Otterlund[10], L.S. Peak[15], N.G. Peresadko[12], N.V. Petrov[16], V.A. Plyushchev[14], W.Y. Qian[18], Y.M. Qin[9], R. Raniwala[6], S. Raniwala[6], N.K. Rao[7], M. Roeper[11], V.V. Rusakova[5], N. Saidkhanov[17], N.A. Salmanova[12], L.G. Sarkisova[19], V.R. Sarkisyan[19], A.M. Seitimbetov[1], G.S. Shabratova[5], C.I. Shakhova[1], S.N. Shpilev[17], D. Skelding[13], K. Söderström[10], Z.I. Solovieva[14], E. Stenlund[10], L.N. Svechnikova[17], M. Tothova[8], M.I. Tretyakova[12], T.P. Trofimova[16], U.I. Tuleeva[16], B.P. Tursunov[16], S. Vokal[8], J. Vrlakova[8], H.Q. Wang[10,18], Z.Q. Weng[4], R.J. Wilkes[13], Y.L. Xia[4], C.B. Yang[18], D.H. Zhang[9], P.Y. Zheng[2], S.I. Zhokhova[17], D.C. Zhou[18], The EMUO1-Collaboration

[1]High Energy Physics Institute, Almaty, Kazakhstan
[2]Institute of High Energy Physics, Academia Sinica, Beijing, China
[3]Department of Physics, Punjab University, Chandigarh, India
[4]Department of Physics, Hunan Education Institute, Changsha, Hunan, China
[5]Laboratory of High Energies, Joint Institute for Nuclear Research (JINR), Dubna, Russia
[6]Department of Physics, University of Rajasthan, Jaipur, India
[7]Department of Physics, University of Jammu, Jammu, India
[8]Department of Nuclear Physics and Biophysics, Safarik University, Kosice, Slovakia
[9]Department of Physics, Shanxi Normal University, Linfen, Shanxi, China
[10]Department of Physics, University of Lund, Lund, Sweden
[11]F.B. Physik, Philipps University, Marburg, Germany
[12]Laboratory of Cosmic Physics, P N Lebedev Physical Institute, Moscow, Russia
[13]Department of Physics, University of Washington, Seattle, Washington, USA
[14]V G Kholpin Radium Institute, St. Petersburg, Russia
[15]Schol of Physics, University of Sydney, Sydney, Australia
[16]Laboratory of Relativistic Nuclear Physics, Institute of Nuclear Physics, Tashkent, Uzbekistan
[17]Laboratory of High Energies, Physical-Technical Institute, Tashkent, Uzbekistan
[18]Institute of Particle Physics, Hua-Zhong Normal University, Wuhan, Hubei, China
[19]Yerevan Physics Institute, Yerevan, Armenia

Received: 28 November 1994

Abstract. The fragmentation topology of ^{28}Si at 3.7A GeV and 14.6A GeV and ^{32}S at 200A GeV in reactions with emulsion nuclei is presented. The fragmentation cross sections are very similar at all three energies. A statistical percolation model can qualitatively describe the data for $Z \geq 6$. The He production is underestimated and the $3 \leq Z \leq 5$ fragments overestimated by this model.

PCAS: 20.25; 75. + r

1. Introduction

In high energy nucleus-nucleus collisions, fragments from the projectile and the target nuclei can be well separated. The process where a part of the nucleus is suddenly liberated is called fragmentation [1] and if the second nucleus acts only as energy injector one denotes it limiting fragmentation [2]. If limiting fragmentation is fulfilled and the sources are well separated in momentum space the study of critical behavioiur by e.g. percolation methods becomes useful.

Attempts have been made to study critical phenomena in nuclear emulsions under the assumption that the projectile fragmentation products can be isolated even in central collisions at 1 A GeV [3] with some positive conclusions concerning a sharp phase transition [4]. Another attempt to use data from central collisions alone and assume initial fusion at energies between 20 A and 200 A MeV also indicates the onset of multifragmentation but not as a sharp transition [5].

The topological structure of the projectile fragmentation of ^{12}C, ^{22}Ne and ^{28}Si nuclei at 3.3 A–3.7 A GeV were studied in Refs. [6–8]. In this paper we discuss the topology for $^{28}Si(^{32}S)$ fragmentation at 3.7 A, 14.6 A and 200 A GeV.

Table 1. The statistics of identified collisions

Projectile energy	3.7 A GeV	14.6 A GeV	200 A GeV
Total number of collisions	1986	955	775
$N_h = 0,1$	443	265	283
$N_h = 2$–7	734	328	234
$N_h \geq 8$	809	362	258
$N(2 \leq N_h \leq 7)/N(N_h \geq 8)$	0.91 ± 0.07	0.91 ± 0.09	0.91 ± 0.12
Events with total destruction of the projectile nucleus ($Z \geq 2$)			
$N_h = 0,1$	75	58	50
$N_h = 2$–7	265	135	80
$N_h \geq 8$	557	273	166
$N(2 \leq N_h \leq 7)/N(N_h \geq 8)$	0.48 ± 0.05	0.49 ± 0.07	0.48 ± 0.09

2. Experimental details

NIKFI BR-2 stacks of nuclear emulsions, 600 μm thick, have been exposed horizontally to the 3.7 A GeV ^{28}Si beam at the DUBNA synchrophasotron, to the 14.6 A GeV ^{28}Si beam of BNL/AGS and to the 200 A GeV ^{32}S beam of the CERN/SPS. Details about scanning and measurements are given elsewhere [9–13].

The event statistics for the three samples are presented in Table 1. N_h stands for the number of charged target fragments defined by range or energy loss in the emulsion ($E_{\text{proton}} < 400$ MeV). Table 1 also shows the number of events with total projectile destruction (TD) defined as those events where only projectile fragments with charge, $Z \leq 2$ remains. The ratio between the number of collisions with $2 \leq N_h \leq 7$ (CNO + peripheral AgBr) and the number of collisions with $N_h \geq 8$ (only AgBr) is independent of the beam energy.

2.1. *The classification of projectile fragments*

At high incident energy nearly all projectile fragments with $Z \geq 2$ have small emission angles and can be well separated from the produced particles and target fragments. All projectile fragments with $Z \geq 3$ and most fragments with $Z = 1$ and $Z = 2$ are emitted within the fragmentation cone defined by a critical angle θ_c; $\theta_c = 1$ mrad at 200 A GeV, $\theta_c = 13$ mrad at 14.6 A GeV and $\theta_c = 44$ mrad at 3.7 A GeV. These values correspond to a spectator proton with a transverse momentum of 200 MeV/c.

The charge of the projectile fragments was determined by δ-ray counting. The following relation was used,

$$N_\delta = A + B \cdot Z^2, \tag{1}$$

where N_δ is the number of δ-rays for 20 mm track length. The values of A and B were determined for each emulsion plate. For light fragments ($Z = 2$–4) complementary gap counting were performed. No differences in N_δ or the gap density was accepted over 20 mm. The accuracy of the Z determination was always better than ± 1 unit. This was verified by summing up the charge of projectile fragments in events of electromagnetic dissociation type.

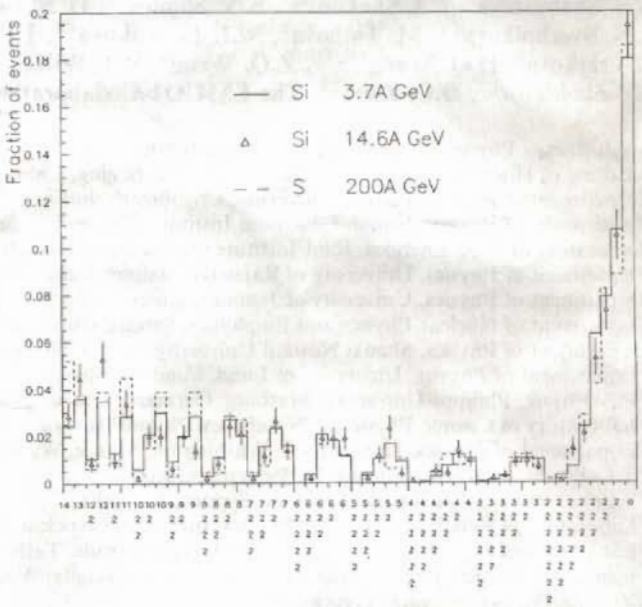

Fig. 1. Topological diagram for $N_h \geq 0$ events. The numbers below x-axis present the fragment charge distribution of the event

3. Results

With the above mentioned criteria for separation and identification of projectile fragments we obtain the topology given in Appendices 1 and 2. In Fig. 1 we show the topology for all events (i.e. $N_h \geq 0$). It should be noticed that the distribution emanating from ^{32}S fragmentation is normalized to the ^{28}Si yield for all channels with $Z \leq 14$. The similarity of the distributions is obvious and the beam energy is of little importance for the nuclear fragmentation process except possibly for the most peripheral interactions. Also the He multiplicity distributions in Fig. 2 are very similar (8 He fragments can of course only be found in ^{32}S breakup). Two kinds of events, discussed also in refs. [6–8], are specially studied; the TD (total disintegration) events and events which have at least one projectile fragment with $Z \geq 3$. Events with two heavy fragments are scarce and their fraction is the same $1.8 \pm 0.2\%$, $1.7 \pm 0.3\%$ and $2.3 \pm 0.5\%$ for 3.7, 14.6 and

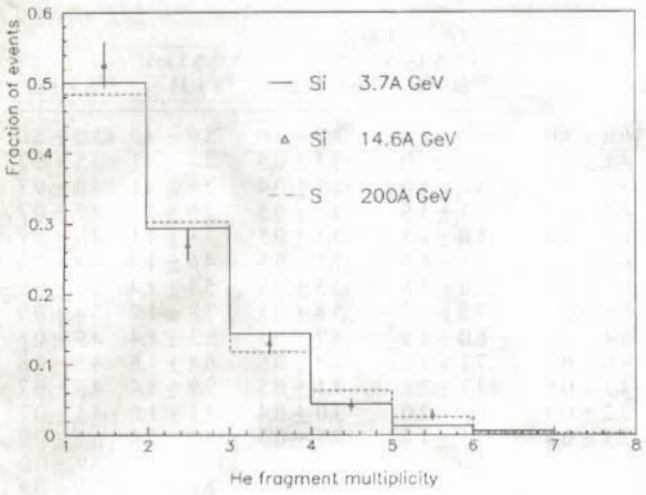

Fig. 2. Multiplicity distribution of He fragments

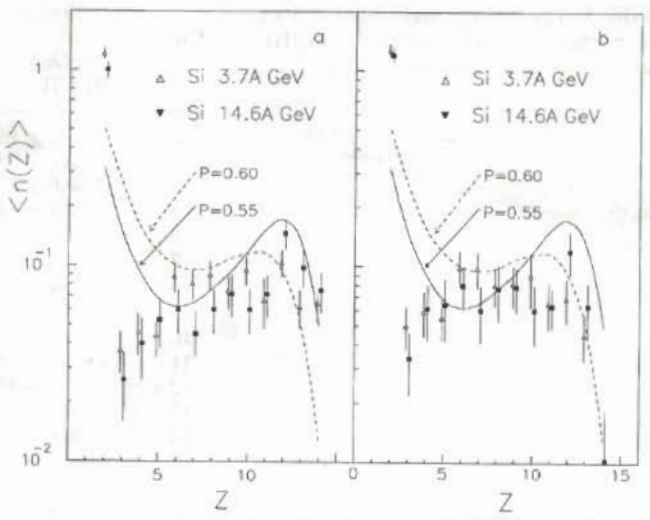

Fig. 3. **a** Charge distribution of the fragments in ^{28}Si interactions of a quasi-nucleon type ($N_h = 0, 1$): **b** after subtraction of electromagnetic dissociation events. The curves are calculated by the bond percolation model with $P = 0.55$ and 0.60

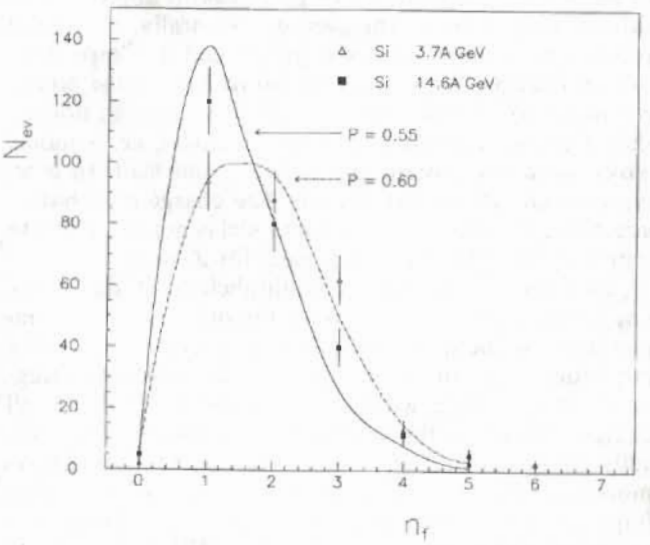

Fig. 4. Multiplicity distribution of the fragments with charge $Z \geq 2$ in interactions of quasi-nucleon type. The *curves* are calculated by the percolation model

200 A GeV respectively. It has been shown in Ref. [13] that the cross-section of TD events should follow a geometrical formula like the one suggested by Bradt and Peters [14] for relativistic (inelastic) nucleus–nucleus interactions,

$$\sigma_{TD} = (1.58\, A_1^{0.026})^2 \cdot (A_1^{1/3} + A_2^{1/3} - 0.85\, A_1^{0.38})^2, \qquad (2)$$

where A_1 and A_2 denote the mass numbers of the colliding nuclei. Table 2 compares the experimental and calculated values. Events with $N_h = 0, 1$ are predominantly "quasi-nucleon" interactions, i.e. interactions with a H nucleus or with only one bound nucleon in CNO or AgBr nuclei. The $N_h = 2$–7 group is dominated by CNO collisions and peripheral AgBr collisions whereas the $N_h \geq 8$ group consists of AgBr interactions with a substantial degree of disintegration. The fraction of TD events is the same within the errors at all three energies and agrees reasonable well with the predictions from Eq. (2). This result indicates that the yield of total destruction of event is energy independent from 4 A GeV to 200 A GeV.

In the second group of events, i.e. those including fragments with $Z \geq 3$, one observes some energy dependence, particularly in the channels with a small degree of disintegration. This comes mainly from the quasi-nucleon ($N_h = 0, 1$) events. In Figs. 3 and 4 we show the charge and the multiplicity distribution of $Z \geq 2$ fragments in interactions of quasi-nucleon type compared to predictions from the bond-percolation prescription [15, 16], in which the nucleus is considered as a cubic lattice where each nucleon has bonds to its nearest neighbours. Only one parameter, p, the probability of breaking a bond $(1 - p)$, is introduced after the dimension of the lattice is set. For ^{28}Si the cubic 3-3-3 lattice is a good approximation. The calculated mass distribution is transformed into a charge distribution by the assumption that all A = 3, 4 isotopes corresponds to $Z = 2$; $A = 5, 6$ isotopes to $Z = 3$ etc. In Figs. 3 and 4 such calculation are shown for $P = 0.55$ and $P = 0.60$. These calculations reproduce well with experimental multiplicity distributions (Fig. 4) and the charge distributions for

Table 2. Fraction of TD events in minimum bias collisions with varioius degree of target breakup. The calculations are based on Eq. (2)

Projectile energy	3.7 A GeV (^{28}Si)	14.6 A GeV (^{28}Si)	Calc.	200 A GeV (^{32}S)	Calc.
$N_h = 0, 1$	$17 \pm 2\%$	$18 \pm 2\%$	21%	$18 \pm 3\%$	18%
$N_h = 2$–7	37 ± 3	40 ± 3	47	35 ± 5	43
$N_h \geq 8$	66 ± 4	71 ± 4	68	65 ± 6	65

Table 3. The average multiplicity (0.100) of fragments in quasi-nuclear events (H) and in minimum-bias events (Em)

Charge	$\langle n_f \rangle$ 0.100					
	3.7 A GeV		14.6 A GeV		200 A GeV	
	^{28}Si + H	^{28}Si + Em	^{28}Si + H	^{28}Si + Em	^{32}S + H	^{32}S + Em
2	121.0 ± 8.0	96.0 ± 3.0	100.0 ± 9.0	98.0 ± 3.0	78.0 ± 3.0	85.0 ± 5.0
3	3.7 ± 0.9	4.1 ± 0.5	2.6 ± 10	3.3 ± 0.5	2.8 ± 1.1	3.5 ± 0.7
4	4.6 ± 1.1	3.8 ± 0.2	4.0 ± 1.4	3.7 ± 0.4	2.8 ± 1.1	4.0 ± 0.7
5	4.4 ± 1.0	4.7 ± 0.5	5.3 ± 1.5	4.2 ± 0.5	2.5 ± 1.0	3.7 ± 0.7
6	8.8 ± 1.5	6.1 ± 0.6	6.0 ± 1.5	5.4 ± 0.5	3.5 ± 1.1	4.8 ± 0.8
7	8.1 ± 1.4	6.0 ± 0.6	4.5 ± 1.3	5.1 ± 0.5	4.6 ± 1.3	4.9 ± 0.8
8	9.0 ± 1.5	6.1 ± 0.6	6.0 ± 1.5	5.5 ± 0.5	5.3 ± 1.4	5.5 ± 0.9
9	7.4 ± 1.4	5.5 ± 0.5	7.2 ± 1.7	5.4 ± 0.5	7.8 ± 1.7	5.4 ± 0.9
10	9.5 ± 1.6	5.4 ± 0.5	6.0 ± 1.5	5.7 ± 0.5	5.3 ± 1.4	4.9 ± 0.8
11	6.7 ± 1.9	4.0 ± 0.5	7.2 ± 1.7	4.4 ± 0.5	6.4 ± 1.6	4.5 ± 0.8
12	10.4 ± 1.6	4.5 ± 0.5	14.7 ± 2.5	4.1 ± 0.5	5.9 ± 1.4	4.3 ± 0.7
13	6.2 ± 1.3	3.2 ± 0.4	9.8 ± 2.0	3.0 ± 0.4	7.1 ± 1.6	3.4 ± 0.7
14	6.5 ± 1.3	2.3 ± 0.3	7.5 ± 1.7	2.5 ± 0.3	14.5 ± 2.4	6.3 ± 0.9
15					12.4 ± 2.2	5.9 ± 0.9
16					6.0 ± 1.5	2.6 ± 0.6
≥3	85.0 ± 6.0	56.0 ± 2.0	82.0 ± 7.0	53.0 ± 3.0	86.0 ± 7.0	64.0 ± 4.0

$Z \geq 5$. Also the rise for $Z = 2$ is predicted but the detailed Z dependence in the region $2 \leq Z \leq 5$ is not well described.

The critical value of p is about 0.75 and hence the best fit for $p \approx 0.55$ indicates that the breakup appears from subcritical systems on the average. Naturally, no kind of pre-foremd α-substructures is introduced in the percolation simulation. Which may be the reason for the underestimation of the He yield. Finally it should be noticed that a one-dimensional percolation model, i.e. a model which does not contain any critical point leads to a binomial multiplicity distribution. The charge distribution generated by such a percolation model is not at all able to reproduce the increase of the yield for $Z = 10$–12.

In Table 3 the average multiplicities of fragments, $\langle n_f \rangle$, with charge Z is given for the minimum bias samples and for the quasi-nucleon events ($N_h = 0,1$). In the minimum bias sample the average multiplicity of fragments is the same within the statistical errors for all charges except for those with $Z = 14$ which are not directly comparable. The yield of He fragments is always more than ten times larger than the yield of any other fragment (nota bene as long as the elastic events are excluded). It has been shown earlier [17] that the ratio beteen He and H fragments decreases as the overlap between the colliding nuclei increases. The cascade evaporatioin model [17] does not account for the existence of such α-structures inside the nuclei and it therefore significantly underestimates the yied of doubly charged fragments. The quasi-nucleon events show a decreasing average number of He fragments with increasing energy while the heaviest fragments may show the opposite tendency. This may however be due to the fact that Table 3 presents the original event sample without any subtraction of ED-events. Data on mean multiplicities after ED-events exclusion are shown in Fig. 3b.

4. Conclusion

In conclusion we find:

i) Limiting fragmentation of the projectile seems to be achieved at 3.7 A GeV.

(ii) The yields of multiply charged fragments are the same at 3.7, 14.6 and 200 A GeV.

iii) For quasi-nucleon target events there is an enhancement of the heaviest fragments. This effect is mainly due to an increase of the ED events.

iv) The multiplicity and charge distributions of fragments with $Z \geq 6$ are qualitatively described by a statistical percolation model for quasi-nucleon events where the size of the fragmenting system is well defined. The α emission channel seems however to be stronger than the prediction while the $3 \leq Z \leq 5$ channels are weaker.

The financial support from the Swedish Natural Science Research Council, The Royal Swedish Academy of Sciences, The International Science Foundation and the Russiar Foundation of Fundamental Research, The Australian Research Council, The German Federal Minister of Research and Technology, The University Grants Commission of the Government of India, The National Science Foundation of China, The Distinguished Teacher Foundation of the State Education Commission of China, The Fok Ying Tung Education and The United States Department of Energy and National Science Foundation is gratefully acknowledged.

Appendix 1

Topology of the ^{28}Si fragmentation at 14.6 A and 3.7 A GeV (minimum bias).

	14.6 A GeV				3.7 A GeV			
N_h	0–1	2–7	≥8	≥0	0–1	2–7	≥8	≥0
Channels								
Si	20	7		27	28	13	6	47
Al + H	26	15	1	42	27	37	6	70
Mg + He	8			8	16	4		20
Mg + 2H	31	15	4	50	29	34	5	68
Na + He + H	7	2		9	15	10		25
Na + 3H	12	18	2	32	14	24	17	55
Ne + 2He	1	1		2	8	2	1	11
Ne + He + H	9	8	2	19	16	18	6	40
Ne + 4H	6	11	2	19	17	27	14	58
F + 2He + H	3	2	1	6	7	10	1	18

Appendix 1 (continued)

	14.6 A GeV				3.7 A GeV			
N_h	0–1	2–7	≥8	≥0	0–1	2–7	≥8	≥0
F + He + 3H	9	7	3	19	13	16	10	39
F + 5H	6	4	3	13	12	29	14	55
O + C					1			1
O + Be + 2H					1			1
O + 3He	1		1	2	2	3	1	6
O + 2He + 2H	4	3	1	8	12	7	2	21
O + He + 4H	6	11	6	23	18	24	10	52
O + 6H	5	8	7	20	5	22	12	39
N + C						1		1
N + B + H						3		3
N + Be + 2H		1		1				
N + Li + 4H	1	1		2				
N + 3He + H	1	1		2	1	3	2	6
N + 2He + 3H	3	5	3	11	11	15	4	30
N + He + 5H	7	10	8	25	19	17	9	45
N + 7H		7	6	13	4	11	16	31
2C + 2H	1			1	1		1	2
C + B + 2He					1			1
C + B + He + H					1	2		3
C + B + 3H				1			1	
C + Be + He + 2H	1			1				
C + Be + 4H							1	
C + Li + He + 3H					1	1	1	3
C + Li + 5H	1			1		1		1
C + 3He + 2H	1	1		2	3	3	1	7
C + 2He + 4H	5	7	6	18	18	16	6	40
C + He + 6H	5	6	7	18	8	14	13	35
C + 8H	3	6	9	18	2	12	8	22
B + Be + He + 3H	1			1		1		1
B + Be + 5H					1	1		2
B + 2Li + 3H		1		1				
B + Li + He + 4H					2			2
B + Li + 6H						2		2
B + 3He + 3H	1		1	2	3	5		8
B + 2He + 5H	2	8	1	11	4	11	5	20
B + He + 7H	9	8	5	22	4	18	10	32
B + 9H	1	2	1	4	2	7	9	18
2Be + He + 4H	1		1	2			1	1
2Be + 6H			1	1			1	1
Be + Li + He + 5H	1			1		1		1
Be + 5He		1		1				
Be + 4He + 2H					1			1
Be + 3He + 4H	3	2		5	2	1	2	5
Be + 2He + 6H	3	1		4	6	5	3	14
Be + He + 8H	1	6	6	13	6	8	9	23
Be + 10H	1	7	1	9	3	7	10	20
2Li + He + 6H						2	2	4
2Li + 8H					1	1		2
Li + 5He + H						1		1
Li + 4He + 3H		2		2			2	2
Li + 3He + 5H	1		2	3	2	1	2	5
Li + 2He + 7H	3	5	1	9	5	5	6	16
Li + He + 9H	1	5	3	9	3	6	11	20
Li + 11H		3	4	7	1	6	12	19
6He + 2H		1		1	5	1		6
5He + 4H	6	6	2	14	4	6	3	13
4He + 6H	4	7	9	20	11	27	8	46
3He + 8H	13	23	14	50	26	45	51	122
2He + 10H	16	19	34	69	16	59	78	153
He + 12H	8	31	60	99	10	66	132	208
14H	5	32	103	140	3	60	227	290
O[1]	1	1	41	43		1	58	59
ALL	265	328	362	955	433	733	809	1975

[1]No fragments inside the cone defined by $\theta \leq \theta_c$

Appendix 2

Topology of the ^{32}S fragmentation at 200 A GeV.

N_h	0–1	2–7	≥8	≥0
Channels				
S	17	3	–	20
P + H	35	10	1	46
Si + He	14	–	–	14
Si + 2H	27	6	2	35
Al + He + H	–	1	–	1
Al + 3H	17	6	2	25
Mg + Li + H	1	–	–	1
Mg + 2He	2	1	–	3
Mg + He + 2H	1	1	2	4
Mg + 4H	11	11	4	26
Na + 2He + H	–	–	–	–
Na + He + 3H	2	–	3	5
Na + 5H	16	9	5	30
Ne + 3He	–	–	–	–
Ne + 2He + 2H	–	1	1	2
Ne + He + 4H	4	4	2	10
Ne + 6H	11	11	4	26
F + 3He + H	1	–	–	1
F + 2He + 3H	1	1	–	2
F + He + 5H	9	3	1	13
F + 7H	11	9	6	26
O + 4He	–	–	–	–
O + 3He + 2H	2	1	–	3
O + 2He + 4H	1	2	–	3
O + He + 6H	7	9	3	19
O + 8H	5	7	6	18
N + Be + He + 3H	–	1	–	1
N + Li + He + 4H	1	–	–	1
N + 4He + H	3	–	–	3
N + 3He + 3H	–	2	1	3
N + 2He + 5H	3	1	1	5
N + He + 7H	5	5	6	16
H + 9H	1	3	5	9
2C + He + 2H	–	1	–	1
C + Be + He + 4H	–	–	1	1
C + Be + 6H	1	–	–	1
C + Li + He + 5H	1	–	–	1
C + 4He + 2H	–	–	–	–
C + 3He + 4H	1	–	–	1
C + 2He + 6H	3	6	2	11
C + He + 8H	2	8	2	12
C + 10H	2	3	3	8
2B + He + 4H	–	1	–	1
2B + 6H	1	1	–	2
B + Be + 2He + 3H	1	–	–	1
B + Be + He + 5H	–	1	–	1
B + Li + He + 6H	–	1	–	1
B + 4He + 3H	–	–	–	–
B + 3He + 5H	–	1	1	2
B + 2He + 7H	2	3	2	7
B + He + 9H	1	1	2	4
B + 11H	1	6	–	7
2Be + He + 6H	–	–	1	1
2Be + 8H	–	–	1	1
Be + Li + 2He + 5H	–	–	1	1
Be + Li + He + 7H	–	1	–	1
Be + 5He + 2H	–	–	–	–
Be + 4He + 4H	–	–	–	–
Be + 3He + 6H	1	1	1	3
Be + 2He + 8H	2	1	5	8
Be + He + 10H	2	–	3	5
Be + 12H	–	2	4	6
2Li + He + 8H	1	–	–	1
Li + 6He + H	–	–	–	–

Appendix 2 (continued)

N_h	0–1	2–7	≥8	≥0
Channels				
Li + 5He + 3H	–	–	–	–
Li + 4He + 5H	–	–	–	–
Li + 3He + 7H	–	–	–	–
Li + 2He + 9H	1	4	2	7
Li + He + 11H	1	4	3	8
Li + 13H	1	–	3	4
8He	–	–	–	–
7He + 2H	1	–	–	1
6He + 4H	–	–	1	1
5He + 6H	7	1	1	9
4He + 8H	6	10	3	19
3He + 10H	8	12	8	28
2He + 12H	6	27	22	55
He + 14H	7	17	35	59
0	15	13	96	124
	283	234	258	775

References

1. Goldhaber, A.S.: Phys. Lett. **47**B, 306 (1974)
2. Heckman, H.H., Greiner, D.E., Lindstrom, P.J., Bieser, F.S.: Phys. Rev. Lett. **28**, 236 (1972)
3. Waddington, C.J., Freier, P.S.: Phys. Rev. C**31** 888 (1985)
4. Campi, X.: Phys. Lett. B**208**, 352 (1988)
5. Jakobsson, B., et al.: Nucl. Phys. A**509**, 195 (1990)
6. Bogdanov, V.G., Plyushchev, V.A., Solovjeva, Z.T.: Leningrad radium institute. (Preprint RI-177 1984)
7. Andreeva, N.P., et al.: JINR Dubna. (Preprint PI-85-692 1985)
8. Krasnov, S.A., et al.: JINR Dubna. (Preprint PI-88-252 1988)
9. Andreeva, N.P., et al.: Yadernaja Physica V**47** 157 (1988)
10. Ameeva, B.U., et al.: Yadernaja Physica V**51** 1047 (1990)
11. Adamovich, M.I., et al.: (EMU01-collaboration), Phys. Lett. **201**B 369 (1991)
12. Adamovich, M.I., et al.: (EMU01-collaboration). Phys. Rev. Lett. **62** 2801 (1989); Mod. Phys. Lett. A**6** 569 (1991).
13. Bogdanov, V.G., et al.: Yadernaja Physica V**47**, 1814 (1988)
14. Bsadt, H.L., Peters, B.: Phys. Rev. **77**, 54 (1950)
15. Bauer, W., et al.: Nucl. Phys. A**152**, 600 (1986)
16. Campi, X.: J. Phys. A: Math. **19** L917 (1986)
17. EL-Naghy., A, et al.: J. Phys. G**80**, 943 (1950); Nucl. Phys. **14**, 1125 (1988)